Role of the helium ground state in $(e,3e)$ processes

L. U. Ancarani, T. Montagnese, and C. Dal Cappello
LPMC, Institut de Physique, Technopôle 2000, 57078 Metz, France
(Received 17 January 2004; revised manuscript received 12 March 2004; published 28 July 2004)

Absolute $(e,3e)$ measurements on helium, at high incident energy, have been recently reproduced by a calculation in the first Born approximation [Phys. Rev. Lett. **91**, 73201 (2003)]. The theoretical model is based on the product of three Coulomb waves for the final state and the use of Pluvinage wave function for the initial helium ground state. The authors suggest that the good agreement obtained is strongly related to the quality of the initial state, in particular to the fact that it is diagonal in all Coulomb interactions. In this paper, we show that this conclusion is not correct. We construct three other helium ground states to demonstrate that diagonalizing the Hamiltonian is not the deciding factor in obtaining agreement with the absolute experimental data.

DOI: 10.1103/PhysRevA.70.012711 PACS number(s): 34.80.Dp

I. INTRODUCTION

Ionization of atoms and molecules by electron impact is one of the fundamental processes of atomic physics. The comprehension of such processes is important for plasma physics and nuclear fusion devices. The study of kinematically complete double ionization experiments by electron impact is a very powerful tool to investigate the role of electron-electron correlation. In the so-called $(e,3e)$ experiments the three electrons (the two ejected and the scattered) are detected in coincidence (see the review paper [1]). These difficult measurements allow us to check with a good accuracy the different theories. Helium is an ideal theoretical target as its final state is a bare nucleus.

The coplanar $(e,3e)$ experiments on helium of Lahmam-Bennani *et al.* [2] have been performed at an incident energy of $\sim$5.6 keV and under a small projectile's scattering angle of 0.45° (momentum transfer of 0.24 a.u.; dipolar regime). The two ejected electrons have been detected with equal energy (10 eV) and absolute angular cross sections have been measured.

Several theoretical description have been proposed for the calculation of $(e,3e)$ cross sections (see Sec. II for more details, and [1] for a review). For the kinematical situation selected in the measurements of Ref. [2], the first Born approximation (FBA)—with respect to the interaction of the fast projectile with the target—should apply [3]; moreover, the 3C model [4,5]—where the final state is described by a product of three Coulomb waves—seems also sufficient. In this paper, we shall restrict the discussion to the 3C model within the FBA.

What remains is the question of what to use for the description of the helium bound state. Hydrogenic and Hylleraas wave functions [6] yield cross sections similar in shape and magnitude, but are in bad agreement [3] with the experimental results. Jones and Madison [3] have therefore suggested using the wave function introduced by Pluvinage [7]. The calculated $(e,3e)$ cross sections are then in overall good agreement (in 16 out of the 20 geometrical situations) with the experimental data of [2]. The authors therefore conclude that this agreement is related to the quality of Pluvinage wave function, in particular because it diagonalizes the Hamiltonian in all three Coulomb singularities. In this contribution, we would like to show that this claim is not correct. The comparison of calculated $(e,3e)$ cross sections obtained with three other helium bound state functions will demonstrate that diagonalizing the Hamiltonian is not the deciding factor in obtaining agreement with the absolute experimental data. We therefore believe that Jones and Madison have made hasty conclusions, since the good agreement with experimental data can be reproduced also with a wave function which does not diagonalize the Hamiltonian.

In Sec. II, we briefly describe the 3C model within the FBA. The choice and properties of several bound state helium wave functions are discussed in Sec. III. Calculated cross sections with these initial state wave functions are compared in Sec. IV. Concluding remarks are given in Sec. V.

II. 3C MODEL FOR $(e,3e)$ CROSS SECTIONS

The fivefold differential cross section (FDCS) corresponding to the $(e,3e)$ reaction,

$$e^- + \mathrm{He} \rightarrow 3e^- + \mathrm{He}^{2+}, \tag{1}$$

is given by

$$\frac{d^5\sigma}{d\Omega_a\, d\Omega_b\, d\Omega_s\, dE_a\, dE_b} = \frac{k_s k_a k_b}{k_i}|T_{fi}|^2, \tag{2}$$

where $d\Omega_s, d\Omega_a$ and $d\Omega_b$ denote, respectively, the elements of the solid angle for the scattered and the two ejected electrons. The energy intervals of the two ejected electrons are represented by dE_a and dE_b. The momenta of incident, scattered, the first and second ejected electrons are denoted, respectively, by k_i, k_s, k_a, and k_b.

The dominant theoretical models used to describe $(e,3e)$ processes are [1] the following.

(i) The 3C model (or BBK model) where the final state is described by a product of three Coulomb waves which account for the interaction between each electron and the nucleus, and for the electron-electron repulsion [4,5]. This double-continuum final state is asymptotically exact. An improvement of the 3C approach consists in using effective

 ©2004 The American Physical Society

charges (model C4FS [2]) for describing the correlated four-body final state.

(ii) The convergent close coupling (CCC) model [8]. This model consists in solving the Lippmann-Schwinger equation for the three-body problem. Technically the double ionization process is identified as an excitation of the positive-energy pseudostate of the ion.

(iii) The Green's function expansion of Ref. [9] which corresponds to the well established Faddeev equations [10] for three particles (it is the lowest order iteration of an incremental approach to the four-body Coulomb problem). The use of this model is, however, limited by numerical difficulties.

(iv) The 6C model [3,11,12] takes into account the pairwise final state interactions between all four particles (the scattered electron, the two ejected electrons and the nucleus). This model corresponds to a product of six Coulomb waves and necessitates a difficult nine-dimensional numerical integral.

As we restrict our study to high incident energies, we shall only use the 3C model within the FBA. This choice is guided by the fact that (i) calculations with electron and positron impact have shown the validity of the FBA [3]; (ii) the 3C model seems sufficient because there is practically no difference between the results of the 3C model and those of the 6C model [3].

When considering high impact energies, it is reasonable to describe the incoming and scattered electrons by plane waves (FBA for the description of the projectile-target interaction). Moreover, since the scattered electron is faster than the ejected electrons, the effect of their exchange can be safely neglected. In the FBA, the matrix element is then [1]

$$T_{fi} = -\frac{1}{2\pi}\langle e^{i\vec{k}_s\vec{r}_0}\Psi_f^-(\vec{r}_1,\vec{r}_2,\vec{k}_a,\vec{k}_b)|V(r_0,r_1,r_2)|\Psi_i(\vec{r}_1,\vec{r}_2)e^{i\vec{k}_i\vec{r}_0}\rangle, \tag{3}$$

where V is the Coulomb interaction between the projectile and the helium atom ($Z=2$),

$$V(r_0,r_1,r_2) = -\frac{Z}{r_0} + \frac{1}{|\vec{r}_0-\vec{r}_1|} + \frac{1}{|\vec{r}_0-\vec{r}_2|} \tag{4}$$

(r_0 is the distance between the incident electron and the nucleus, r_1, r_2 are the distances between one of the helium electron and its nucleus). In Eq. (3), $\Psi_i(\vec{r}_1,\vec{r}_2)$ is the initial bound state of helium. The final state in the 3C model is described by a symmetrized product of three Coulombic distortion factors (one for each two-body Coulomb interaction) [4,5],

$$\Psi_f^-(\vec{r}_1,\vec{r}_2,\vec{k}_a,\vec{k}_b) = \frac{1}{\sqrt{2}}[\varphi(\vec{k}_a,\vec{r}_1)\varphi(\vec{k}_b,\vec{r}_2) + \varphi(\vec{k}_a,\vec{r}_2)\varphi(\vec{k}_b,\vec{r}_1)] \times\chi(|\vec{k}_a-\vec{k}_b|,\vec{r}_{12}), \tag{5}$$

with

$$\varphi(\vec{k},\vec{r}) = \frac{1}{(2\pi)^{3/2}}e^{\pi\eta/2}\Gamma(1+i\eta)e^{i\vec{k}\vec{r}}{}_1F_1(-i\eta,1,-i(kr+\vec{k}\vec{r})), \tag{6}$$

where $\eta=Z/k$ and ${}_1F_1$ is the confluent hypergeometric function. The term $\chi(|\vec{k}_a-\vec{k}_b|,\vec{r}_{12})$ takes into account the repulsion between the two ejected electrons,

$$\chi(|\vec{k}_a-\vec{k}_b|,\vec{r}_{12}) = e^{-\pi\eta_{ab}/2}\Gamma(1-i\eta_{ab}) \times{}_1F_1(i\eta_{ab},1,-i(k_{ab}r_{12}+\vec{k}_{ab}\vec{r}_{12})), \tag{7}$$

where $\eta_{ab}=1/|\vec{k}_a-\vec{k}_b|$ and $\vec{k}_{ab}=(\vec{k}_a-\vec{k}_b)/2$.

The final double-continuum state Ψ_f^- and the initial ground state Ψ_i are, in principle, orthogonal because they are eigenfunctions of the same Hamiltonian. However, since in each case we do not know the exact solutions, any approximation will break the orthogonality. The latter can be restored by an artificial orthogonalization through

$$\langle\Psi_f^{-\perp}| = \langle\Psi_f^-| - \langle\Psi_f^-|\Psi_i\rangle\langle\Psi_i|. \tag{8}$$

If this operation leads to important corrections in the cross sections, it indicates that the model possibly breaks down.

For the calculation of the nine-dimensional integral (3), we first use the Bethe transformation for the integration over r_0,

$$\frac{e^{i\vec{k}\vec{a}}}{k^2} = \frac{1}{4\pi}\int\frac{e^{i\vec{k}\vec{r}}}{|\vec{r}-\vec{a}|}d\vec{r}, \tag{9}$$

to reduce it to a six-dimensional integral over $\vec{r}_1$ and $\vec{r}_2$,

$$T_{fi} = -\frac{2}{K^2}\langle\Psi_f^-(\vec{r}_1,\vec{r}_2,\vec{k}_a,\vec{k}_b)|e^{i\vec{K}\vec{r}_1}+e^{i\vec{K}\vec{r}_2}-Z|\Psi_i(\vec{r}_1,\vec{r}_2)\rangle, \tag{10}$$

where $\vec{K}=\vec{k}_i-\vec{k}_s$ is the momentum transfer.

When the initial state Ψ_i is described by a Hylleraas-type function $e^{-\alpha r_1}e^{-\beta r_2}r_{12}^n e^{-\gamma r_{12}}$, the calculation of the matrix element T_{fi} can be reduced to a double numerical integration (see details in [4,5]).

When the Pluvinage wave function is used [see Eq. (24c), next section], we have been able to reduce the six-dimensional integral to a three-dimensional numerical (Gauss-Legendre) quadrature—instead of a six-dimensional numerical quadrature as in [3]. To do this, we first replace the confluent hypergeometric function of Pluvinage wave function with parameter k by using the transformation (13.2.1) of [13],

$${}_1F_1\left(1-\frac{i}{2k},2,2ikr_{12}\right) = \frac{\Gamma(2)}{\Gamma\left(1+\frac{i}{2k}\right)\Gamma\left(1-\frac{i}{2k}\right)}\int_0^1 e^{2ikr_{12}t}t^{-i/2k}(1-t)^{i/2k}\,dt, \tag{11}$$

so that the matrix element becomes

$$T_{fi} = -N_P \frac{2}{K^2} \frac{\Gamma(2)}{\Gamma\left(1+\frac{i}{2k}\right)\Gamma\left(1-\frac{i}{2k}\right)} \int_0^1 t^{-i/2k}(1-t)^{i/2k}\, dt \times \int e^{-Zr_1} e^{-Zr_2} e^{ikr_{12}(2t-1)} \Psi_f^{-*}(\vec{r}_1,\vec{r}_2,\vec{k}_a,\vec{k}_b) \times (e^{i\vec{K}\vec{r}_1} + e^{i\vec{K}\vec{r}_2} - Z) d\vec{r}_1\, d\vec{r}_2. \quad (12)$$

The six-dimensional integral appearing in (12) can be reduced to a linear combination of several two-dimensional integrals as indicated in detail in the appendices of [4,5]. Hence, the calculation of the matrix element is reduced to a sum of three-dimensional integrations.

III. HELIUM GROUND STATE WAVE FUNCTION

Jones and Madison [3] have claimed that the good agreement of their theoretical calculations with experimental $(e,3e)$ data is directly related to the quality of the Pluvinage wave function for the helium bound state, in particular because it diagonalizes the Hamiltonian in all three Coulomb singularities. In this section, we shall analyze some properties of this and other initial state wave functions to check whether this is true.

Let us start with the nonrelativistic Schrödinger equation (SE) for the helium atom $(Z=2)$, in which we neglect the nucleus mass effects. Let r_1 and r_2 be the two electrons radial coordinate, and $r_{12}=|\vec{r}_1-\vec{r}_2|$ the electron-electron distance. Considering S-states only (and in particular the $^1S_0$ ground state), the six-dimensional SE reduces to the well known three-dimensional Hylleraas equation (HE). The latter is expressed as

$$H\Psi(r_1,r_2,r_{12}) = E\Psi(r_1,r_2,r_{12}), \quad (13)$$

where the Hamiltonian H can be written as

$$H = H_1 + H_2 + H_{12} + H'_{12}, \quad (14)$$

with

$$H_i = -\frac{1}{2}\left(\frac{\partial^2}{\partial r_i^2} + \frac{2}{r_i}\frac{\partial}{\partial r_i}\right) - \frac{Z}{r_i} \quad (i=1,2), \quad (15a)$$

$$H_{12} = -\left(\frac{\partial^2}{\partial r_{12}^2} + \frac{2}{r_{12}}\frac{\partial}{\partial r_{12}}\right) + \frac{\alpha}{r_{12}}, \quad (15b)$$

$$H'_{12} = -\frac{r_1^2 - r_2^2 + r_{12}^2}{2r_1 r_{12}}\frac{\partial^2}{\partial r_1\, \partial r_{12}} - \frac{r_2^2 - r_1^2 + r_{12}^2}{2r_2 r_{12}}\frac{\partial^2}{\partial r_2\, \partial r_{12}}. \quad (15c)$$

In H_{12}, the quantity α is introduced to "turn on" $(\alpha=1)$ or "switch off" $(\alpha=0)$ the electron-electron interaction; no analytical solution exists today for Eq. (13) for the physical situation $(\alpha=1)$. Note that three singularities (i.e., $r_1=0, r_2=0$ or $r_{12}=0$) appear in H, and the factors multiplying the mixed partial derivatives in H'_{12} are always finite.

The mean energy,

$$E = \frac{\langle\Psi|H|\Psi\rangle}{\langle\Psi|\Psi\rangle}, \quad (16)$$

is usually minimized with trial wave functions (variational method). The energy, which can be considered as *numerically exact*, of the $^1S_0$ ground state of (13) is $E_{exact} = -2.903724$ a.u. [14].

Let us define the local energy [15],

$$E(r_1,r_2,r_{12}) = \frac{1}{\Psi(r_1,r_2,r_{12})} H\Psi(r_1,r_2,r_{12}). \quad (17)$$

Only for the exact solution, this local energy will be a constant throughout the entire configuration space, i.e., an eigenvalue of (13), and hence equal to the mean energy [this is the case, for example, for the hydrogenic ions of nuclear charge Z, for which the local and mean energies are equal to $E = -Z^2/2n^2$ (a.u.)]. For any other trial wave function, the local energy will not be a constant value; the averaging over the whole space [see Eq. (16)] smooths out the variations of the local energy and provides a finite constant value as close as possible to the numerically exact value. For the study of collisions with a helium atom, it is necessary to have a good wave function and not only a good mean energy (the latter is enough for spectroscopical purposes). Obtaining a good mean energy is not a sufficient criterion to state that a trial wave function is good [16]. Having an almost constant local energy is a much stronger quality test.

Bartlett [15] has shown that Hylleraas wave functions provide local energies ranging from $-\infty$ to ∞. Infinite local energies can come from two sources: (i) the wave function has nodes and $H\Psi \neq 0$; (ii) one or several of the singularities of the potential terms in H_1, H_2 and H_{12} (i.e., $r_1=0, r_2=0$ or $r_{12}=0$) are not compensated by the corresponding kinetic terms. The study of the singularities has led Kato [17] to provide mathematical conditions that Ψ must satisfy (the so-called "cusp conditions") in order to eliminate these singularities:

$$\left[\frac{\partial\overline{\Psi}}{\partial r_1}\right]_{r_1\to 0} = -Z\Psi(0,r_2,r_{12}), \quad (18a)$$

$$\left[\frac{\partial\overline{\Psi}}{\partial r_2}\right]_{r_2\to 0} = -Z\Psi(r_1,0,r_{12}), \quad (18b)$$

$$\left[\frac{\partial\overline{\Psi}}{\partial r_{12}}\right]_{r_{12}\to 0} = \frac{1}{2}\Psi(r,r,0), \quad \text{with} \quad r = \frac{1}{2}\left|(\vec{r}_1 + \vec{r}_2)\right|, \quad (18c)$$

where $\overline{\Psi}$ means the average of Ψ over a very small sphere of radius r_1 (respectively, r_2 or r_{12}) keeping the other values fixed. Relations (18a)–(18c) provide the linear behavior that Ψ must have close to the singularity points.

If the electron-electron interaction is neglected $(\alpha=0)$, r_{12} is no longer needed in Ψ. The exact solution of (13) is the product of two hydrogenic $He^+(1s)$ functions $e^{-Z(r_1+r_2)}$, which yields the mean or local energy $-Z^2$. Of course, in the

physical case $\alpha=1$, Ψ will depend also on r_{12} and the electronic structure of the helium ground state is substantially modified. A first approach is to consider wave functions of the kind

$$f(r_1)f(r_2)h(r_{12}), \tag{19}$$

where $h(r_{12})$ is a correlation function (note that, for the ground state, Ψ is symmetric in r_1, r_2). The product (19), however, can never be the solution of (13) since the equation is not separable in the three variables r_1, r_2, r_{12} because of the presence of H'_{12}.

For the purpose of the present study, let us ignore the H'_{12} term of the Hamiltonian (this term has no singularity). This corresponds to replacing the three-body system to 3 two-body systems; Eq. (13) is then fully separable and the solution can be written as in (19). Building up from the $\alpha=0$ solution, let us consider the hydrogenic functions $f(r_i)=e^{-Zr_i}$, and $h(r_{12})$ an eigenfunction of H_{12}. The latter are exact solutions of the well known Coulomb-type differential equation (without centrifugal term, $L=0$)

$$\left[-\left(\frac{\partial^2}{\partial r_{12}^2}+\frac{2}{r_{12}}\frac{\partial}{\partial r_{12}}\right)+\frac{\alpha}{r_{12}}\right]g(r_{12})=\varepsilon g(r_{12}), \tag{20}$$

and are given by the Coulomb-type functions [13] with either a positive ($\varepsilon>0$) or negative ($\varepsilon<0$) eigenvalue. Considering only regular solutions at $r_{12}=0$, we have

$$g_+(r_{12})=e^{-kr_{12}}{}_1F_1\left(1+\frac{\alpha}{2k},2,2kr_{12}\right), \quad \text{with} \quad \varepsilon=-k^2<0, \tag{21a}$$

$$g_-(r_{12})=e^{-ikr_{12}}{}_1F_1\left(1-i\frac{\alpha}{2k},2,2ikr_{12}\right), \quad \text{with} \quad \varepsilon=k^2>0, \tag{21b}$$

where k is a real number (note that, because of Kummer's relations [13], k and $-k$ give the same solutions); both $g_+(r_{12})$ and $g_-(r_{12})$ are real functions of r_{12}. The first **(**$g_+(r_{12})$**)** correspond to bound solutions (in the sense of negative energy) while the second **(**$g_-(r_{12})$**)** to continuum solutions. Hence, the wave function (19),

$$e^{-Zr_1}e^{-Zr_2}g_\pm(r_{12}) \tag{22}$$

is a product of three Coulomb functions and is analogous to the 3C final state in (5). Each of the two-body Coulomb interactions for the bound state is treated exactly and hence the Kato cusp conditions (18a)–(18c) are automatically satisfied.

If we ignore H'_{12}, the exact separable solution (22) yields a local (and mean) energy of

$$E=-Z^2\mp k^2. \tag{23}$$

In the case of the bound solutions $g_+(r_{12})$, we have a special situation when $1+1/2k=-N$ where $N>0$ is an integer. Indeed, the confluent hypergeometric function reduces then to a Laguerre polynomial of order N, i.e., $L_N^1(kr_{12})/(N+1)$ [13] and $g_+(r_{12})$ to a hydrogenic function (exponential times a polynomial). The use of a correlation function $h(r_{12})$ in the form of an exponential times a polynomial has been used in many trial wave functions (e.g., [6,18,19]). However, usually, the parameters appearing in both the exponential and in the polynomial are chosen in order to optimize the mean energy rather than to eliminate the singularity of the potential term $1/r_{12}$, and hence satisfy Kato's cusp condition (18c).

In the calculations of $(e,3e)$ cross sections which we will present in the next section, we shall consider four bound state wave functions corresponding to four different correlation functions $h(r_{12})$. The first three are of the family (22), i.e., separable solutions which automatically satisfy Kato cusp conditions. Two of them, Ψ_0 and Ψ_1, are $g_+(r_{12})$ functions corresponding, respectively, to $N=0$ ($k_0=-1/2$) and $N=1$ ($k_1=-1/4$). A third one, Ψ_P, is a $g_-(r_{12})$ function corresponding to the value $k=k_P=0.410$ which minimizes the mean energy (this is Pluvinage choice [7] as used by Jones and Madison [3]). The fourth one, Ψ_A, has a $h(r_{12})$ function which is not solution of (20) and is mathematically similar to the correlation factor of Le Sech function [19] but with the numbers of Ψ_1. The normalized wave functions, with the corresponding mean energies are

$$\Psi_0=N_0e^{-Z(r_1+r_2)}e^{(1/2)r_{12}}, \quad E_0=-2.8561 \text{ a.u.}, \tag{24a}$$

$$\Psi_1=N_1e^{-Z(r_1+r_2)}e^{(1/4)r_{12}}\left(1+\frac{r_{12}}{4}\right), \quad E_1=-2.8721 \text{ a.u.}, \tag{24b}$$

$$\Psi_P=N_P\,e^{-Z(r_1+r_2)}e^{-ikr_{12}}{}_1F_1\left(1-i\frac{1}{2k},2,2ikr_{12}\right), \quad E_P=-2.8788 \text{ a.u.}, \tag{24c}$$

$$\Psi_A=N_Ae^{-Z(r_1+r_2)}\left(1+e^{(1/4)r_{12}}\frac{r_{12}}{4}\right), \quad E_A=-2.8766 \text{ a.u.} \tag{24d}$$

where $N_0=1.343$, $N_1=1.429$, $N_P=1.535$ and $N_A=1.797$. These four wave functions have comparable mean energies which are not so good when compared to the values obtained with other wave functions available in the literature. In the best case, the Ψ_P wave function yields only about 40% of the correlation energy, which is defined to be the difference between E_{exact} and the Hartree-Fock energy. However, their analytical forms are simple, and practical for collision calculations. Higher order Laguerre polynomials can be easily envisaged, but they provide only a slight improvement to the mean energy (of the order of 0.0033 a.u. at most) at the cost of a slightly longer analytical form.

Let us now describe some of the properties of the first three functions Ψ_0, Ψ_1 and Ψ_P which are exact separable solutions. The corresponding correlation functions $h(r_{12})$ with the normalization factors as given in (24a)–(24c) are plotted in Fig. 1 as a function of r_{12}. They are regular at $r_{12}=0$, but behave quite differently at asymptotic distances ($r_{12}\to\infty$). For Ψ_0 and Ψ_1, $h(r_{12})$ increases at large distances while, for Ψ_P, it tends to zero in an oscillatory way. The Pluvinage function Ψ_P has therefore an infinite number of

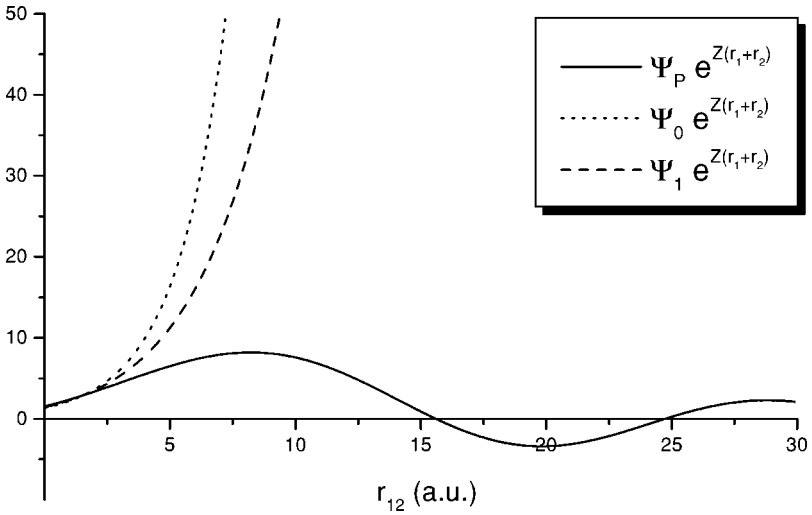

FIG. 1. Behavior of Ψ_0 (dotted line), Ψ_1 (dashed line), and Ψ_P (solid line) multiplied by $e^{Z(r_1+r_2)}$ as a function of r_{12}.

nodes, although for large value of r_{12} only. Note that none of the three wave functions has the correct global three-body asymptotic behavior [20].

Since the electron-electron interaction is repulsive it makes sense, at a first glance, to believe that a continuum wave function $g_-(r_{12})$ for $h(r_{12})$ is a better choice than a bound solution $g_+(r_{12})$. Indeed, the former contributes with a positive (rather than negative) energy, and hence provides a local energy (23) closer to the exact value. This, however, will not be necessarily true when the full Hamiltonian is considered since the operator H'_{12} mixes the variables r_1, r_2 and r_{12}, and the local energy is not constant anymore.

Another argument seemingly in favor of the continuum solution is that the function goes asymptotically ($r_{12}\to\infty$) to zero in one case and increases to infinity in the other (see Fig. 1). One must not forget, however, that the exponential terms $e^{-Z(r_1+r_2)}$ will dominate the large distance behavior ensuring that the function (22) will represent a bound state. Indeed, when r_{12} is large, either r_1 or r_2, or both must also be large; as long as it does not increase exponentially faster than $e^{Zr_{12}}$, $h(r_{12})$ does not need, therefore, to go to zero at large distances. Moreover, the correlation function $h(r_{12})$ represents the influence of the electron-electron interaction, but does not necessarily represent a physical bound state on its own. Let us remind that the helium three-body system cannot be reduced to the product of 3 two-body systems.

One of the arguments put forward in the paper of Jones and Madison [3] is that Ψ_P diagonalizes the Hamiltonian in all Coulomb interactions. By construction, both Ψ_0 and Ψ_1 have the same property. As stated in [3], the remaining term in the Hamiltonian, H'_{12}, does not have singularities. However, since the Pluvinage wave function Ψ_P has nodes (see Fig. 1), the contribution of H'_{12} to the local energy (17) has an infinite number of infinite values. This is exactly one of the deficiencies of Hylleraas wave functions as pointed out by Bartlett [15] and quoted by [3]. The wave functions Ψ_0 and Ψ_1, on the contrary, do not have any nodes, and provide a local energy finite everywhere. This will be illustrated below.

In summary, when comparing the properties of the three wave functions (24a)–(24c), Ψ_0 and Ψ_1 should not be inferior to the Pluvinage wave function Ψ_P, except possibly for the value of the mean energy.

The fourth wave function, Ψ_A is given by (24d); the corresponding correlation function has no nodes and behaves very similarly to that shown in Fig. 1 for Ψ_1 (the dominant asymptotic term is the same). The function Ψ_A is not a separable solution, so that it does not diagonalize the Hamiltonian in all Coulomb singularities and does not satisfy Kato's cusp condition (18c). In this respect, Ψ_A should be a much worse representation of the helium ground state than the previous three wave functions.

Some of the properties of the four wave functions can be illustrated by comparing their local energies (17). The variation with respect to the exact numerical value may be represented by the quantity $\delta E = E(r_1,r_2,r_{12}) - E_{exact}$: small values of δE are a sign that a wave function behaves well locally. For illustration purposes, we have chosen to select, in the three dimensional space (r_1,r_2,r_{12}), the following situations: $r_2 = 5r_1$ (Fig. 2) and $r_2 = 1$ a.u. (Fig. 3). In each case the mutual angle $\theta_{12} = \arccos[(r_1^2 + r_2^2 - r_{12}^2)/(2r_1r_2)]$ is fixed, and δE is plotted versus r_1. The same vertical scale is used in both figures and, to avoid overloading them, we consider only Ψ_1, Ψ_P and Ψ_A.

In Fig. 2, when r_1 tends to zero, the variables r_2 and r_{12} tend to zero as well because $r_2 = 5r_1$. A singularity in δE appears for Ψ_A, but not for Ψ_1 and Ψ_P: this is directly related to the fact that Ψ_A does not satisfy the Kato cusp condition (18c), while Ψ_1 and Ψ_P do. At larger values of r_1, δE tends to a finite value for Ψ_1 and Ψ_A, whereas it varies enormously for Ψ_P with divergences at the corresponding nodes of $h(r_{12})$ (see Fig. 1). Note that, in all cases, δE is finite for Ψ_1.

In Fig. 3, r_2 is fixed at 1 a.u. For the special case $\theta_{12} = 0$, the operator H'_{12} gives no contribution to the local energy. For the separable solutions Ψ_1 and Ψ_P, the local energy is exactly constant, as given by (23): by construction, δE is smaller for Ψ_P than for Ψ_1. For Ψ_A, on the other hand, δE is not constant. A singularity appears for $r_1 = 1$ a.u., i.e., when $r_{12}\to 0$, which corresponds to the failure in satisfying the Kato cusp condition (18c). For $\theta_{12} = 0.5\pi$ and $\theta_{12} = \pi$, δE is finite for Ψ_1 and Ψ_A, with reasonable asymptotic values. For

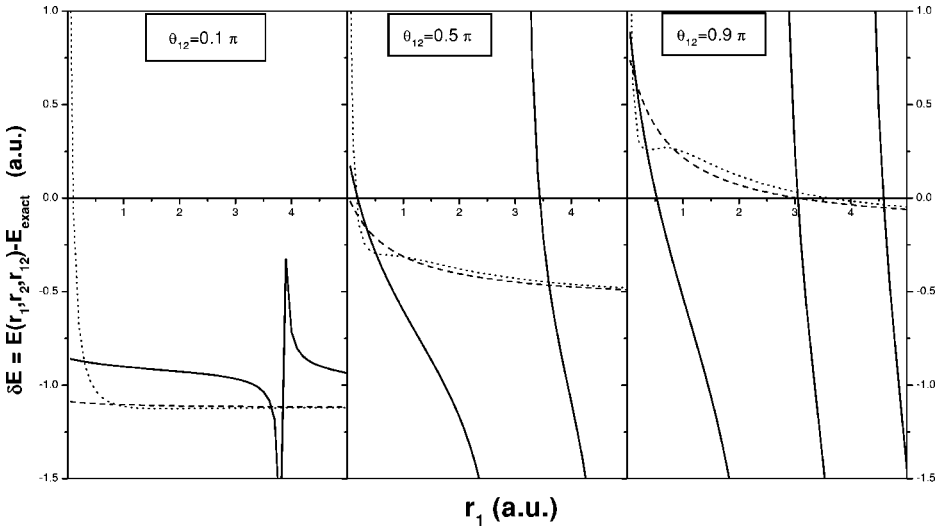

FIG. 2. Variation of $\delta E = E(r_1, r_2, r_{12}) - E_{exact}$ obtained for Ψ_A (dotted line), Ψ_1 (dashed line), and Ψ_P (solid line). δE is plotted as a function of r_1, for $r_2 = 5r_1$ and for three values of the mutual angle θ_{12}: 0.1 π (left panel), 0.5 π (middle panel), and 0.9 π (right panel).

Ψ_P, on the other hand, δE is finite at short distances but decreases rapidly, and presents a singularity (not shown) when r_{12} takes the value corresponding to the first node of $h(r_{12})$, at about $r_{12} \simeq 16$ a.u. (see Fig. 1).

The situations selected in the three-dimensional space, presented in Figs. 2 and 3, illustrate some of the deficiencies of the wave functions considered, in particular the δE infinite values found for Ψ_P and Ψ_A (these singularities disappear when calculating the mean energy). From this point of view, the comparison also seems to indicate that Ψ_1 yields a local energy which is overall better than Ψ_P and Ψ_A, although Ψ_1 produces a slightly worse mean energy.

In the next section, we shall compare the cross sections calculated with the four wave functions Ψ_0, Ψ_1, Ψ_P, and Ψ_A.

IV. NUMERICAL RESULTS

All fivefold differential cross sections presented here have been calculated with the 3C model in the first Born approximation (as described in Sec. II), but with different bound state helium wave functions Ψ_i in (3). Our calculations with the Pluvinage wave function Ψ_P agree perfectly with the calculations of [3]; note that the numerical approaches differ since we use a three-dimensional quadrature (see the end of Sec. II).

We start by comparing cross sections with the absolute measurements of [2] where all angles are measured in the same sense with respect to the incident beam direction. For illustration purposes, we have selected four ejected angles θ_a, out of the 20 presented in [2] (calculations at other ejected angles have been done and give the same conclusions). Two of them correspond to the direction of the momentum transfer $\theta_a = 319^\circ$ and its opposite $\theta_a = 139^\circ$; the results obtained with Ψ_P are good [3]. In the other two cases $\theta_a = 83^\circ$ and $\theta_a = 207^\circ$; the results of [3] are not in good agreement. The cross sections are plotted as a function of the angle of one of the ejected electrons (θ_b) while the other is fixed (θ_a). For comparison purposes, the same scale (in a.u.) is used in Figs. 4–7.

In Fig. 4 we compare the cross sections obtained with three Hylleraas-type initial wave functions for the helium ground state: Bonham and Kohl — number 7 [18] ($E = -2.8757$ a.u.; with radial correlation only), Bonham and Kohl—number 19 [18] ($E = -2.9035$ a.u.; with radial and angular correlations) and Le Sech [19] ($E = -2.9020$ a.u.).

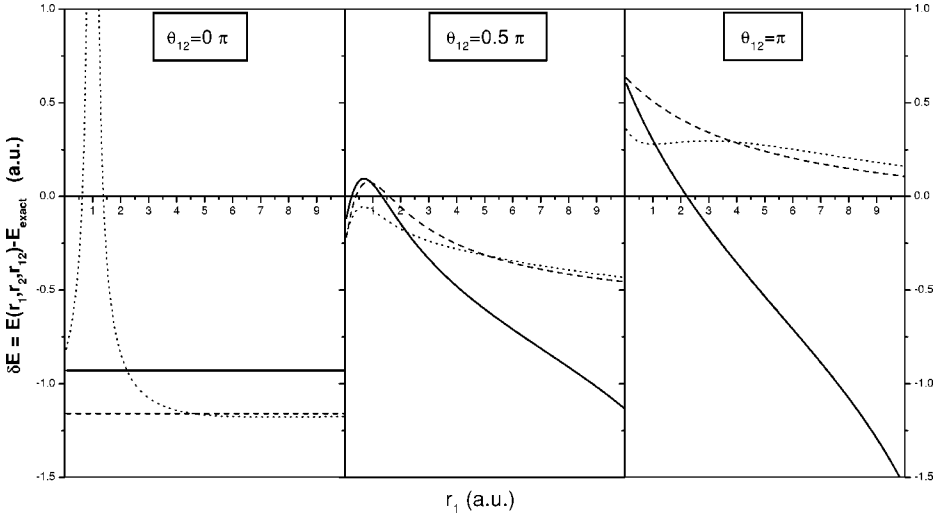

FIG. 3. The same as Fig. 2 but for $r_2 = 1$ a.u. and for three values of the mutual angle θ_{12}: 0 π (left panel), 0.5 π (middle panel) and π (right panel).

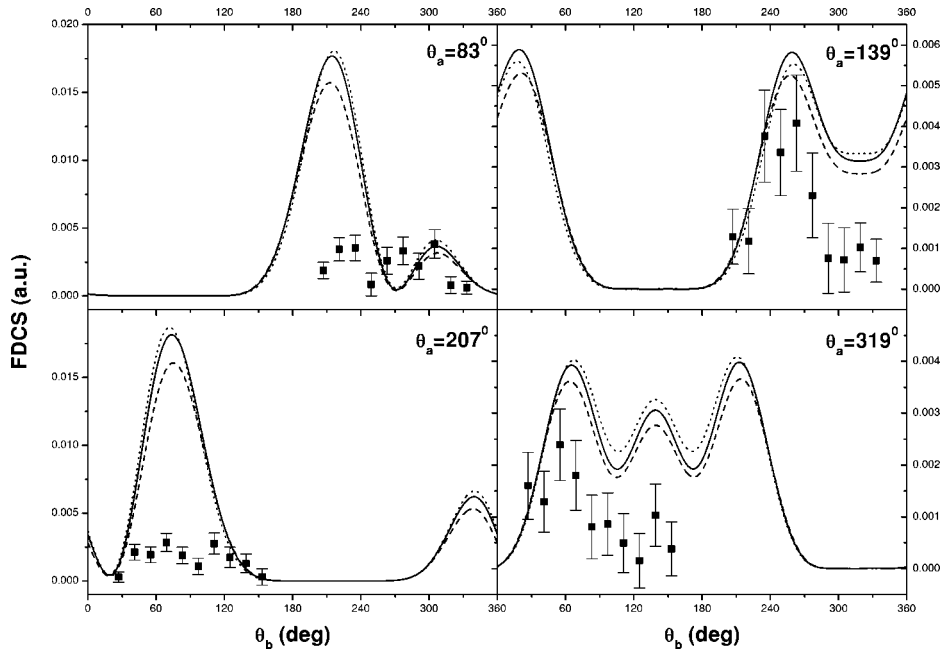

FIG. 4. Fivefold differential cross section (FDCS) for $(e,3e)$ ionization of the helium ground state, as a function of the angle of one of the ejected electrons θ_b. The incident electron (at ~5.6 keV) is scattered at 0.45° and the other ejected electron is detected at θ_a which is indicated in each box. The two ejected electrons escape with equal energy (10 eV). The absolute experimental data [2]: full squares. The three curves are obtained with the 3C model but with different initial wave functions for the helium ground state: Bonham and Kohl — number 7 [18] (dotted line), Bonham and Kohl—number 19 [18] (dashed line) and Le Sech [19] (solid line).

The results obtained with these wave functions yield similar shapes and magnitudes, the curves being bunched together. The magnitude is about a factor 2 larger and thus clearly in disagreement with experimental data. As noted in [3], this is quite different from the factor 10 found in [2] with a three-parameter Hylleraas wave function (note that in the kinematics considered, the use of effective charges rather than integer charges plays only a minor role). We would like to point out that the Le Sech wave function [19] can be considered, in some respects, as an improvement of the original Pluvinage wave function since (i) it introduces a screening in both the electron-electron and in the electron-nucleus interaction; (ii) it satisfies the Kato's cusp conditions; (iii) yields a much better mean energy (with 96% of the correlation energy).

We have also performed calculations with the simple hydrogenic (Slater) wave function ($e^{-\alpha(r_1+r2)}$ with the effective charge $\alpha=27/16$): the cross sections (not shown) have a

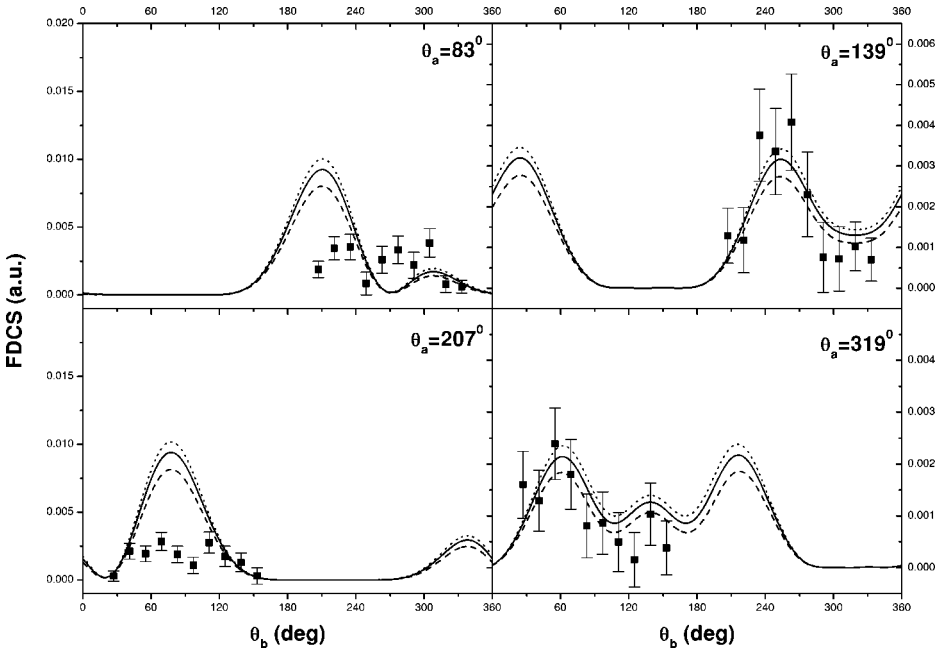

FIG. 5. The same as in Fig. 4, but with the Pluvinage wave function for the helium ground state, corresponding to three different values of k (see the text): $k=0.31$ (dotted line), $k=k_P=0.41$ (solid line), and $k=0.51$ (dashed line).

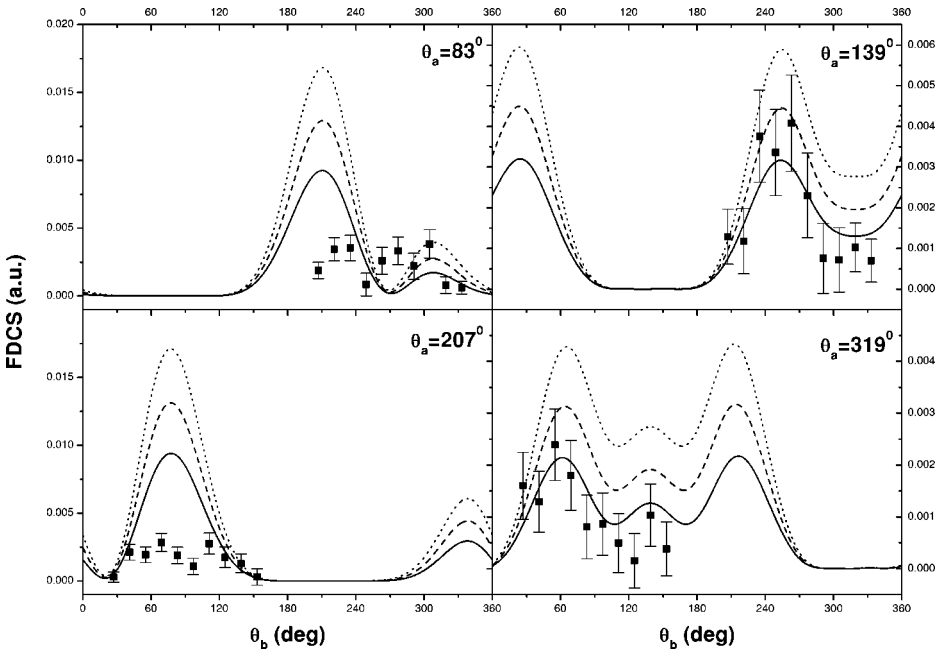

FIG. 6. The same as in Fig. 4, but with different initial wave functions for the helium ground state: Ψ_0 (dotted line), Ψ_1 (dashed line), and Ψ_P (solid line).

similar shape to those shown in Fig. 4, but with a magnitude only about 1.5 larger than the experiments, as indicated in [3].

In Fig. 5 we present the cross sections (solid curve) obtained with Ψ_P given by (24c); they coincide with those published by [3]. We observe that the shapes are essentially similar to those of Fig. 4, but the magnitude is lowered by a factor 2, thus giving the good agreement with experimental data found in 16 out of the 20 geometrical situations [3] (as stated earlier, this agreement is shown here only for $\theta_a = 319^\circ$ and $\theta_a = 139^\circ$). We have also studied the sensitivity to the parameter k in (24c), by comparing the results obtained with $k=0.31$ (dotted curve) and $k=0.51$ (dashed curve). We observe that a small variation of k, which yields only a tiny difference in the mean energy ($E_P[k=0.31] = -2.8783$ a.u., $E_P[k=0.51] = -2.8778$ a.u.), produces a relatively important change in the magnitude of the cross sections. Such sensitivity on a parameter is rarely seen with other trial wave functions.

The cross sections obtained with the three wave functions Ψ_0 (dotted line), Ψ_1 (dashed line) and Ψ_P (solid line), are presented in Fig. 6. We immediately observe that the results with Ψ_0 give a similar disagreement in magnitude with the experimental data as those shown in Fig. 4. On the other hand, the use of Ψ_1 yields cross sections, similar in shape, but with a magnitude which is intermediate between those obtained with Ψ_0 and Ψ_P [21]. From Fig. 6, it clearly appears that, when Ψ_P gives good agreement ($\theta_a = 319^\circ$ and $\theta_a = 139^\circ$), the two wave functions Ψ_0 and Ψ_1 do not. Jones and Madison [3] relate the agreement in magnitude obtained

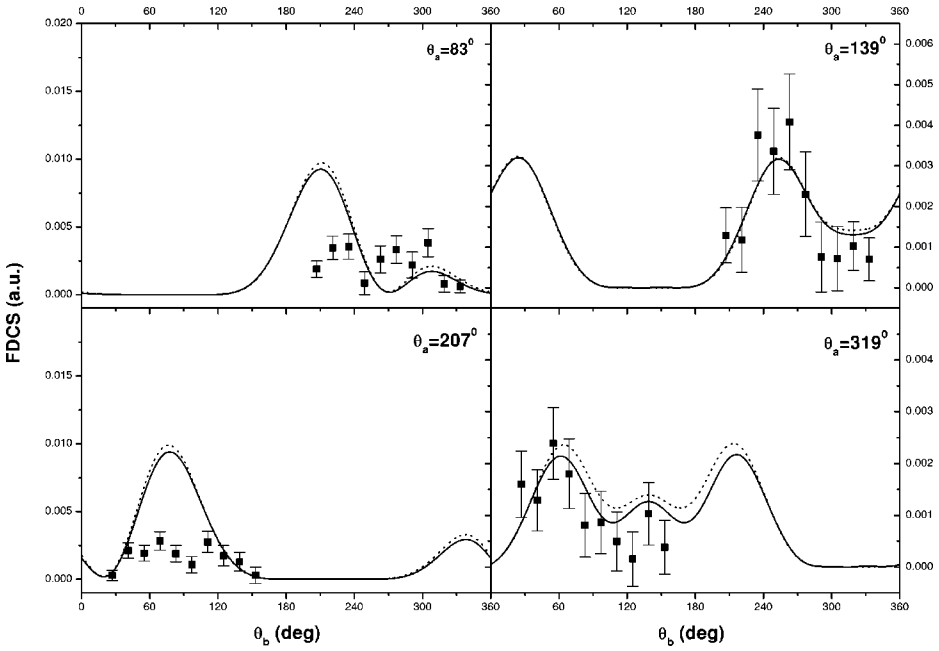

FIG. 7. The same as in Fig. 4, but with different initial wave functions for the helium ground state: Ψ_A (dotted line) and Ψ_P (solid line).

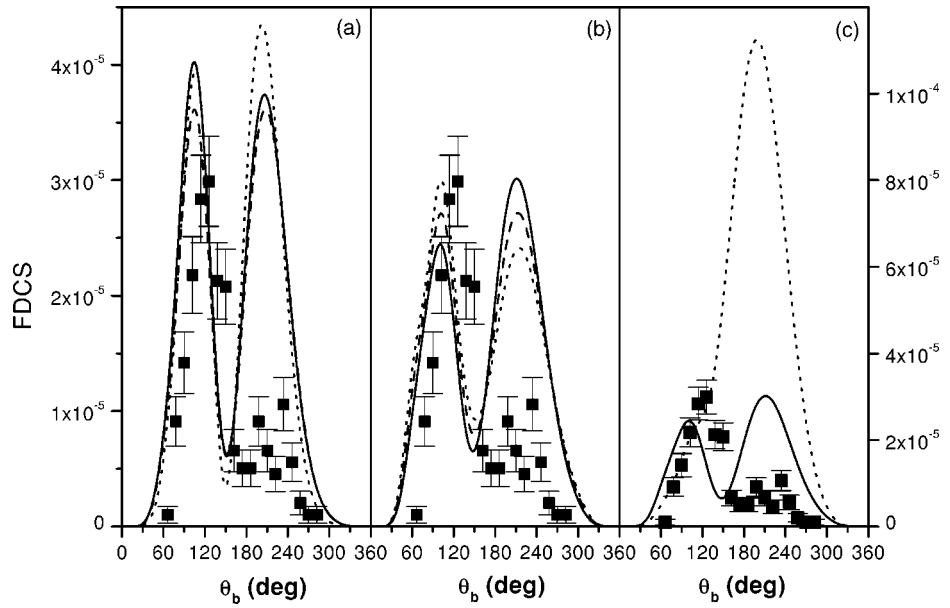

FIG. 8. Fivefold differential cross section (FDCS) for $(e,3e)$ ionization of the helium ground state, as a function of the angle of one of the ejected electrons θ_b. The incident electron (at 2 keV) is scattered at -9.428° and the other ejected electron is detected at $\theta_a=0^\circ$. The two ejected electrons escape with equal energy (25 eV). The relative experimental data [22]: full squares. All curves are obtained with the 3C model but with different initial wave functions for the helium ground state. Panel (a) Bonham and Kohl—number 7 [18] (dotted line); Bonham and Kohl—number 19 [18] (dashed line); and Le Sech [19] (solid line). Panel (b) [the same scale as panel (a)]: Ψ_0 (dotted line), Ψ_1 (dashed line) and Ψ_P (solid line). Panel (c): Ψ_P (solid line) and Ψ_P without orthogonalizing as in Eq. (8) (dotted line).

with the function Ψ_P to the fact that the latter describes the region of space—where the two electrons are close together—better than the Hylleraas-type wave function. Indeed, Ψ_P satisfies the cusp conditions, but so do the wave function proposed by Le Sech [19], and the separable solutions Ψ_0 and Ψ_1. One could then argue that the Le Sech wave function does not diagonalize the Hamiltonian in the three Coulomb singularities, but Ψ_0 and Ψ_1 do so by construction. The results obtained with Ψ_0 and Ψ_1 presented in Fig. 6 indicate therefore that the agreement with experimental data *cannot* be related to the fact that the initial helium wave function diagonalizes the Hamiltonian.

We have also calculated the corresponding cross sections with the function Ψ_A. The results are compared in Fig. 7 to those obtained with Ψ_P. It is clear that there is very little difference between the two sets of results (this is valid for all 20 experimental situations [2]). This figure therefore clearly demonstrates that agreement with experimental data within the 3C model can be obtained also with a wave function which—in principle—cannot be considered as good as the Pluvinage wave function (see details in Sec. III).

Jones and Madison [3] conclude their letter with the following: "*Consequently, electron-electron correlation is treated precisely (and the cusp conditions of Kato are satisfied exactly) by both our initial and final target wave functions and we found that this is crucial for reproducing the absolute measurements.*" Although we agree that treating electron-electron correlation precisely is crucial, we believe that this conclusion is somewhat too hasty. Indeed, the results presented in Figs. 6 and 7 clearly show that (i) a wave function (e.g., Ψ_0 or Ψ_1) which diagonalizes the Hamiltonian does not necessarily reproduce the magnitude of the experimental data; (ii) a wave function (e.g., Ψ_A) which does not diagonalize the Hamiltonian is able to do it. This may be considered as the main result of this paper.

Let us now briefly discuss the influence of orthogonalizing the final state Ψ_f^- to the initial state Ψ_i [see Eq. (8)]. For all the initial state wave functions considered above, the magnitude changes by about 10–15% (as stated in [3]), but the shape is not affected (result not shown). From this point of view, we may thus consider the 3C model to be satisfactory in these geometries and kinematics.

Before concluding, let us consider now the relative $(e,3e)$ measurements of Dorn *et al.* [22] at 2 keV incident energy, where the two ejected electrons escape with equal energy (25 eV), and the scattered electron is detected at -9.428° (momentum transfer of 2 a.u.; impulsive regime). At this incident energy, the use of the 3C model within the FBA should also be justified. The calculated cross sections are presented in Fig. 8 and compared to the relative data as published in [22]. On the left panel (a) are shown the results obtained with the same three Hylleraas-type wave functions considered in Fig. 4: the agreement is poor as the experimental peak ratio is not reproduced. The 3C results published in [22] also fail to reproduce this ratio, but are in sharp contrast with ours. In the middle panel (b) we present the cross sections obtained with Ψ_0, Ψ_1 and Ψ_P, on the same scale as in (a). The results obtained with Ψ_1 and Ψ_P are clearly not in agreement with the experimental data; the results are even worse than those [see panel (a)] obtained with the Hylleraas-type wave functions. The cross section obtained with Ψ_0, on the other hand, is relatively in better agreement, with a better ratio of the two peaks. From this figure the conclusion would not be in favor of Ψ_1 and Ψ_P, but rather of Ψ_0. Similarly to

what is shown in Fig. 7, the cross sections obtained with Ψ_A are almost identical to those obtained with Ψ_P (result not shown). The analysis of these results would lead to different conclusions than those reached before. The comparison of theoretical cross sections with experimental data of Dorn *et al.*, however, cannot provide valid conclusions. Indeed, although 2 keV can be considered as sufficiently high incident energy in order to apply the FBA, the 3C model does not seem to be applicable for these experimental geometry and kinematics (also see the paper [23] where the dependence on the momentum transfer is discussed): the orthogonalization of the final state Ψ_f^- to the initial state Ψ_i gives large spurious contributions. For all initial state wave functions, the cross sections without orthogonalization are very different, with the right-hand side peak a factor 3 to 4 times larger and the left-hand side peak becoming a shoulder; the shape is then similar to the 3C result published in [22]. This is illustrated on the right panel, (c), in the case of Ψ_P. It is interesting to notice that the CCC model gives a good agreement with the relative experimental data of Dorn *et al.* [22] and with those of Lahmam-Bennani *et al.* [2] but it is not able to reproduce its magnitude (factor 3) [24].

V. CONCLUDING REMARKS

In this paper we have critically analyzed the recent agreement with experimental data obtained by FBA calculations based on the 3C model and the use of the Pluvinage wave function, Ψ_P, for the initial helium bound state [3]. We have constructed three other initial state wave functions: two with similar properties (Ψ_0 and Ψ_1) and one which is different (Ψ_A). Keeping the 3C model, the comparison of calculated $(e,3e)$ cross sections with absolute experimental data shows that the conclusions of Jones and Madison are not correct. The demonstration is build on the following two arguments: (i) we have compared the cross sections obtained with three bound state wave functions (Ψ_0, Ψ_1 and Ψ_P) which are such that the Hamiltonian is diagonal in all three Coulomb interactions, and hence satisfy Kato's cusp conditions. Only one of them, the Pluvinage wave function Ψ_P, gives good overall agreement with experimental data; (ii) on the other hand, the wave function Ψ_A which does not have the same properties yields results as good as those published by Jones and Madison [3] with the Pluvinage wave function Ψ_P. It is then clear that the fact that the bound state wave function diagonalizes the Hamiltonian *is not* the deciding factor in obtaining agreement with the absolute experimental data. Certainly, satisfying Kato's cusp conditions is a mathematical requirement of the Schrödinger equation, while making the Hamiltonian diagonal is only one way of removing the Coulomb singularities. Both these properties, however, are not enough to fully deal with the complete Hamiltonian because of the presence of the (nondiagonal, H'_{12}) term which mixes the variables r_1, r_2 and r_{12}: the three-body system cannot be reduced to the product of three two-body systems.

For double ionization processes, treating the electron-electron correlation precisely is certainly crucial. It would be interesting to make an analysis similar to the present one in the case of double photoionization and simultaneous ionization-excitation by electron impact.

ACKNOWLEDGMENTS

The authors would like to thank A. Dorn and A. Lahmam-Bennani for providing experimental data, and the CINES for providing computing time.

[1] J. Berakdar, A. Lahmam-Bennani, and C. Dal Cappello, Phys. Rep. **374**, 91 (2003).
[2] A. Lahmam-Bennani *et al.*, Phys. Rev. A **59**, 3548 (1999).
[3] S. Jones and D. H. Madison, Phys. Rev. Lett. **91**, 073201 (2003).
[4] M. Brauner, J. Briggs, and H. Klar, J. Phys. B **22**, 2265 (1989).
[5] B. Joulakian, C. Dal Cappello, and M. Brauner, J. Phys. B **25**, 2863 (1992).
[6] E. A. Hylleraas, Z. Phys. **48**, 469 (1928) **54**, 347 (1929); **65**, 759 (1930).
[7] P. Pluvinage, Ann. Phys. (Paris) **5**, 145 (1950); J. Phys. Radium **12**, 789 (1951).
[8] I. Bray and A. T. Stelbovics, Phys. Rev. A **46**, 6995 (1992).
[9] J. Berakdar, Phys. Rev. Lett. **85**, 4036 (2000).
[10] L. D. Faddeev, Sov. Phys. JETP **12**, 1014 (1961).
[11] A. W. Malcherek and J. S. Briggs, J. Phys. B **30**, 4419 (1997).
[12] J. R. Götz, M. Walter, and J. S. Briggs, J. Phys. B **36**, L77 (2003).
[13] *Handbook of Mathematical Functions*, edited by M. Abramowitz and I. A. Stegun (Dover, New York, 1972).
[14] G. W. F. Drake, Phys. Scr. **T83**, 83 (1999).
[15] J. H. Bartlett, J. J. Gibbons, and C. G. Dunn, Phys. Rev. **47**, 679 (1935); J. H. Bartlett, *ibid.* **98**, 1067 (1955).
[16] L. U. Ancarani and Y. V. Popov, in *Correlations, Polarization, and Ionization in Atomic Systems*, edited by D. H. Madison and M. Schulz (AIP, New York, 2002), p. 115.
[17] T. Kato, Commun. Pure Appl. Math. **10**, 151 (1957).
[18] R. A. Bonham and D. A. Kohl, J. Chem. Phys. **45**, 2471 (1966).
[19] C. Le Sech, J. Phys. B **30**, L47 (1997).
[20] Yu. V. Popov and L. U. Ancarani, Phys. Rev. A **62**, 042702 (2000).
[21] Other wave functions Ψ_N corresponding to higher order Laguerre polynomials $L_N^1(kr_{12})$ (with $N \geqslant 2$) have been considered. The calculated cross sections are very close to those obtained with Ψ_1.
[22] A. Dorn *et al.*, in *Electron and Photon Impact Ionization and Related Topics 2002*, edited by L. U. Ancarani (IOP, Bristol, 2003), p. 41.
[23] A. S. Kheifets *et al.*, J. Phys. B **35**, L15 (2002).
[24] A. S. Kheifets *et al.*, J. Phys. B **32**, 5047 (1999).